

# Million-Fold Acceleration of a Diels–Alder Reaction due to Combined Lewis Acid and Micellar Catalysis in Water

Sijbren Otto,<sup>†</sup> Jan B. F. N. Engberts,<sup>\*,†</sup> and Jan C. T. Kwak<sup>‡</sup>

Contribution from the Department of Organic and Molecular Inorganic Chemistry, University of Groningen, Nijenborgh 4, 9747 AG Groningen, The Netherlands, and Department of Chemistry, Dalhousie University, Halifax, NS, Canada B3H 4J3

Received May 12, 1998

**Abstract:** The effect of micelles of sodium dodecyl sulfate (SDS), cetyltrimethylammonium bromide (CTAB), dodecyl heptaoxyethylene ether (C<sub>12</sub>E<sub>7</sub>), and copper and zinc didodecyl sulfate (M(DS)<sub>2</sub>) on the Diels–Alder reaction of 3-(para-substituted phenyl)-1-(2-pyridyl)-2-propen-1-ones **1a–g**, containing neutral, cationic, or anionic substituents, with cyclopentadiene (**2**) has been studied. In the absence of catalytically active transition-metal ions, micelles invariably retard the reaction. This can be rationalized on the basis of different binding locations of the reaction partners in the micelle. These binding sites have been probed using solubilize-induced aromatic shifts in the <sup>1</sup>H NMR spectrum of the surfactant and paramagnetic counterion-induced relaxation enhancements of the <sup>1</sup>H NMR signals of the solubilize. In contrast to SDS, CTAB, and C<sub>12</sub>E<sub>7</sub>, Cu(DS)<sub>2</sub> micelles catalyze the Diels–Alder reaction between **1** and **2** with extremely high efficiency, leading to rate enhancements up to 1.8 × 10<sup>6</sup> compared to the uncatalyzed reaction in acetonitrile. This results primarily from the essentially complete complexation of **1** to the copper ions at the micellar surface. Analysis of substituent effects and endo/exo ratios of the Diels–Alder adducts indicates that the reaction experiences a waterlike environment.

## Introduction

The Diels–Alder reaction is an important tool in synthetic organic chemistry, forming the key step in the preparation of many six-membered rings. Many procedures have been developed to increase the yields and selectivities of Diels–Alder reactions.<sup>1</sup> In particular, the discovery that Lewis acids can catalyze these reactions in organic solvents had a large impact on synthetic organic chemistry.<sup>2</sup> The mechanism by which Lewis acids influence the rate and selectivity of the Diels–Alder reaction can be readily explained in terms of the frontier molecular orbital (FMO) theory.<sup>3</sup> For a normal electron demand Diels–Alder reaction, the rate and selectivity depend on the efficiency of the interaction of the HOMO of the diene with the LUMO of the dienophile. Raising the energy of the diene HOMO and lowering the energy of the dienophile LUMO increases the mutual overlap. Therefore, most dienophiles carry an electron-withdrawing substituent to lower their LUMO energy. Coordination of a Lewis acid to this group leads to a further dramatic enhancement of its electron-withdrawing capacity, thereby magnifying its effect on rate as well as on selectivity.

Since 1980, another important impulse in Diels–Alder chemistry came from the discovery of the special effect of water on the Diels–Alder reaction.<sup>4</sup> Accelerations of up to 12 800 times on going from an organic solvent to water have been reported.<sup>5</sup> Synthetic applications of the increase in rate and also

selectivity by this solvent followed promptly.<sup>6</sup> Computer simulations and detailed kinetic studies on the effect of water on a multitude of Diels–Alder reactions have clearly demonstrated that two important properties of this solvent give rise to the dramatic accelerations.<sup>5,7</sup> *Hydrogen-bonding interactions* between water and the activating group of the dienophile accounts for part of the rate enhancement. The mode of action is analogous to Lewis acid catalysis. The remainder of the acceleration can be attributed to *enforced hydrophobic interactions*.<sup>8</sup> The reaction in water is facilitated by the favorable expulsion of water molecules from the hydrophobic hydration shells of the reacting molecules upon approaching the transition state. The relative contributions of hydrogen-bonding and enforced hydrophobic interactions in the aqueous acceleration depend on the character of the diene and the dienophile.<sup>7h</sup>

We have recently reported the first example of a Diels–Alder reaction that benefits from both Lewis acid catalysis and the special effects of water simultaneously, leading to high selectivities and accelerations up to 250 000 times.<sup>9</sup> Herein we show

(5) (a) Otto, S.; Blokzijl, W.; Engberts, J. B. F. N. *J. Org. Chem.* **1994**, *59*, 5372. (b) Engberts, J. B. F. N. *Pure Appl. Chem.* **1995**, *67*, 823.

(6) See: Grieco, P. A. *Organic Synthesis in Water*; Blacky Academic and Professional: London, 1998; and references therein.

(7) (a) Blake, J. F.; Jorgensen, W. L. *J. Am. Chem. Soc.* **1991**, *113*, 7430. (b) Blake, J. F.; Dongchul, L.; Jorgensen, W. L. *J. Org. Chem.* **1994**, *59*, 803. (c) Jorgensen, W. L.; Blake, J. F.; Lim, D.; Severance, D. L. *J. Chem. Soc., Faraday Trans.* **1994**, *90*, 1727. (d) Blokzijl, W.; Engberts, J. B. F. N. In *Structure and Reactivity in Aqueous Solution*; ACS Symposium Series 568; Cramer, C. J., Truhlar, D. G. Eds.; American Chemical Society: Washington, DC, 1994; p 303. (e) van der Wel, G. K.; Wijnen, J. W.; Engberts, J. B. F. N. *J. Org. Chem.* **1996**, *61*, 9001. (f) Furlani, T. R.; Gao, J. *J. Org. Chem.* **1996**, *61*, 5492. (g) Wijnen, J. W.; Engberts, J. B. F. N. *J. Org. Chem.* **1997**, *62*, 2039. (h) Wijnen, J. W. Ph.D. Thesis, University of Groningen, 1997.

(8) (a) Blokzijl, W.; Blandamer, M. J.; Engberts, J. B. F. N. *J. Am. Chem. Soc.* **1991**, *113*, 4241. (b) Blokzijl, W.; Engberts, J. B. F. N. *J. Am. Chem. Soc.* **1992**, *114*, 5440.

<sup>†</sup> University of Groningen.

<sup>‡</sup> Dalhousie University.

(1) Pindur, U.; Lutz, G.; Otto, C. *Chem. Rev.* **1993**, *93*, 741.

(2) Yates, P.; Eaton, P. *J. Am. Chem. Soc.* **1960**, *82*, 4436.

(3) (a) Woodward, R. B.; Hoffmann, R. *Angew. Chem.* **1969**, *81*, 797.

(b) Fukui, K. *Acc. Chem. Res.* **1971**, *4*, 57.

(4) Breslow, R.; Rideout, D. C. *J. Am. Chem. Soc.* **1980**, *102*, 7816.

that even higher rate enhancements of the aqueous Lewis acid-catalyzed Diels–Alder reaction can be achieved through micellar catalysis. Before embarking on a detailed analysis of micelle-catalyzed Diels–Alder reactions, it is appropriate to briefly summarize the basic features of micellar catalysis.

When relatively apolar compounds are introduced in an aqueous micellar solution, dipolar and hydrophobic interactions will cause them to bind to or be taken up by micelles.<sup>10</sup> The solubilization of these compounds is usually treated in terms of the pseudophase model, regarding the bulk water phase as one phase and the micellar pseudophase as another. The affinity of the solubilize for the micelle can then be quantified by a partition coefficient  $P$ . In this article, we will express  $P$  as the ratio of the concentration of the solubilize in the micellar pseudophase divided by the concentration of the solubilize in the aqueous phase.

There has been controversy over the time-averaged location of different solubilizes in or at the micelle.<sup>11</sup> The binding site strongly depends on the nature and concentration of the solubilize as well as the nature of the surfactant. However, some general comments can be made. Polar and ionic groups will preferentially stay at the surface of the micelle, whereas saturated unsubstituted hydrocarbons will reside in the micellar interior.<sup>11a,i,12</sup> Aromatic hydrocarbons are usually located at the interface between the Stern region and the hydrocarbon chains.<sup>11</sup> This has been attributed to the weak hydrogen bond-accepting capabilities of aromatic rings,<sup>13</sup> to the weak surface activity of these compounds, which is amplified by the high surface-to-volume ratio of a micellar solution<sup>14</sup> and, for ammonium surfactants, to specific cation– $\pi$  interactions.<sup>15</sup>

A micelle-bound substrate will experience a medium different from that of bulk water, leading to a kinetic medium effect. Micellar catalysis of organic reactions in water has been reviewed extensively.<sup>16</sup>

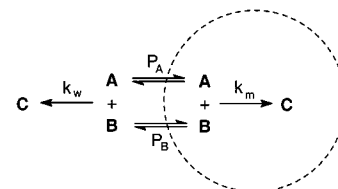


**Figure 1.** Kinetic analysis of a bimolecular reaction  $A + B \rightarrow C$  according to the pseudophase model.

The present work deals with micellar catalysis of bimolecular and termolecular processes. Following the pioneering work of Berezin,<sup>17</sup> using the pseudophase model, the kinetics of these processes can be accounted for by taking into account the individual partition coefficients of both reaction partners and separate rate constants for reaction in the micellar and in the aqueous phase (Figure 1). Determination of the rate constant in the micellar pseudophase generally requires independent assessment of at least one of the involved partition coefficients.<sup>17b</sup> The kinetics of a large number of bimolecular micelle-catalyzed processes have been analyzed in this way.<sup>16</sup> In the majority of cases studied, at least one of the reaction partners is ionic, so that competition in binding with the surfactant counterions has to be taken into account. Romsted et al.<sup>18</sup> have developed the pseudophase ion-exchange model for dealing with these ionic bimolecular reactions. Examples of bimolecular reactions involving two nonionic reactants have been reported.<sup>19</sup> The effect of micelles on the observed rates of all these bimolecular reactions originates from two distinct effects: (a) the medium effect, the reaction partners will experience a different local environment, so that  $k_m$  is different from  $k_w$ ; (b) the local concentration effect, the concentrations of both reaction partners in the micellar pseudophase will be different from those in bulk water. One of the most remarkable observations is that, for nearly all nonionic as well as ionic bimolecular processes, the second-order rate constant for reaction in the micellar pseudophase  $k_m$  virtually equals the rate constant for reaction in the aqueous phase  $k_w$ .<sup>16f,19c,20</sup> Hence, the significant accelerations in terms of the *observed* rates of many bimolecular reaction should be attributed primarily to the increased local concentrations of both reaction partners in the micelle or, more precisely, at the micellar surface.

There are only a few documented examples of micellar catalysis of Diels–Alder reactions.<sup>21</sup> Jaeger<sup>22</sup> has employed orientational effects in micelles to promote the regioselectivity of a Diels–Alder reaction of a surfactant diene and a surfactant dienophile. Recently, Diego-Castro and Hailes studied the influence of sodium dodecyl sulfate (SDS) and cetyltrimethylammonium bromide (CTAB) on the endo/exo selectivity of the Diels–Alder reactions of a range of acrylate esters with cyclopentadiene.<sup>23</sup> Kinetic studies by several authors have

(9) (a) Otto, S.; Engberts, J. B. F. N. *Tetrahedron Lett.* **1995**, *36*, 2645. (b) Otto, S.; Bertocin, F.; Engberts, J. B. F. N. *J. Am. Chem. Soc.* **1996**, *118*, 7702.

(10) (a) Bunton, C. A.; Sepulveda, L. *J. Phys. Chem.* **1979**, *83*, 680. (b) Abraham, M. H.; Chadha, H. S.; Dixon, J. P.; Rafols, C.; Treiner, C. *J. Chem. Soc., Perkin Trans. 2* **1995**, 887. (c) Quina, F. H.; Alonso, E. O.; Farah, J. P. S. *J. Phys. Chem.* **1995**, *99*, 11708.

(11) (a) Eriksson, J. C.; Gillberg, G. *Acta Chem. Scand.* **1966**, *20*, 2019. (b) Arrington, P. A.; Clouse, A.; Doddrell, D.; Dunlap, R. B.; Cordes, E. H. *J. Phys. Chem.* **1970**, *74*, 665. (c) Rehfeld, S. J. *J. Phys. Chem.* **1971**, *75*, 3905. (d) Fendler, J. H.; Patterson, L. K. *J. Phys. Chem.* **1971**, *75*, 3907. (e) Fendler, J. H.; Fendler, E. J.; Infante, G. A.; Shih, P.; Patterson, L. P. *J. Am. Chem. Soc.* **1975**, *97*, 89. (f) Mukerjee, P.; Cardinal, J. R.; Desai, N. R. *Micellization, Solubilization and Microemulsions*; Mittal, K. L., Ed.; Plenum Press: New York, 1977; p 241. (g) Cardinal, J. R.; Mukerjee, P. *J. Phys. Chem.* **1978**, *82*, 1614. (h) Mukerjee, P.; Cardinal, J. R. *J. Phys. Chem.* **1978**, *82*, 1620. (i) Nagarajan, R.; Chaiko, M. A.; Ruckenstein, E. *J. Phys. Chem.* **1984**, *88*, 2916. (j) Kandori, K.; McGreevy, R. J.; Schechter, R. S. *J. Phys. Chem.* **1989**, *93*, 1506.

(12) Jobe, D. J.; Reinsborough, V. C.; White, P. J. *Can. J. Chem.* **1982**, *60*, 279.

(13) (a) Yoshida, Z.; Osawa, E. *J. Am. Chem. Soc.* **1965**, *87*, 1467. (b) Ruelle, P.; Buchmann, M.; Nam-Tran, H.; Kesselring, U. W. *J. Comput. Aided Mol. Des.* **1992**, *6*, 431.

(14) Shobba, J.; Srinivas, V.; Balasubramanian, D. *J. Phys. Chem.* **1989**, *93*, 17.

(15) (a) Hirose, C.; Sepulveda, L. *J. Phys. Chem.* **1981**, *85*, 3689. (b) Lianos, P.; Viriot, M.; Zana, R. *J. Phys. Chem.* **1984**, *88*, 1098. (c) Malliaris, A.; Le Moigne, J.; Sturm, J.; Zana, R. *J. Phys. Chem.* **1985**, *89*, 2709.

(16) (a) Cordes, E. H.; Dunlap, R. B. *Acc. Chem. Res.* **1969**, *2*, 329. (b) Cordes, E. H.; Gitler, C. *Prog. Bioorg. Chem.* **1972**, *2*, 1. (c) Fendler, J. H.; Fendler, E. J. *Catalysis in Micellar and Macromolecular Systems*; Academic Press: New York, 1975. (d) Bunton, C. A. *Pure Appl. Chem.* **1977**, *49*, 969. (e) Cordes, E. H. *Pure Appl. Chem.* **1978**, *50*, 617. (f) Bunton, C. A. *Catal. Rev. Sci. Eng.* **1979**, *20*, 1. (g) Südholter, E. J. R.; van de Langkruis, G. B.; Engberts, J. B. F. N. *Recl. Trav. Chim. Pays-Bas* **1980**, *99*, 73. (h) Kunitake, T.; Shinkai, S. *Adv. Phys. Org. Chem.* **1980**, *17*, 435. (i) Engberts, J. B. F. N. *Pure Appl. Chem.* **1992**, *64*, 1653. (j) Tascioglu, S. *Tetrahedron* **1996**, *52*, 11113.

(17) (a) Yatsimirski, A. K.; Martinek, K.; Berezin, I. V. *Tetrahedron* **1971**, *27*, 2855. (b) Berezin, I. V.; Martinek, K.; Yatsimirskii, A. K. *Russ. Chem. Rev.* **1973**, *42*, 787.

(18) Bunton, C. A.; Nome, F.; Quina, F. H.; Romsted, L. S. *Acc. Chem. Res.* **1991**, *24*, 357.

(19) (a) Heitmann, P. *Eur. J. Biochem.* **1968**, *5*, 305. (b) Bunton, C.; Robinson, L. *J. Am. Chem. Soc.* **1970**, *92*, 356. (c) Tagaki, W.; Amada, T.; Yamashita, Y.; Yano, Y. *J. Chem. Soc., Chem. Commun.* **1972**, 1131. (d) Dougherty, S. J.; Berg, J. C. *J. Colloid Interface Sci.* **1974**, *49*, 135. (e) Jaeger, D. A.; Wegrzyn Clennan, M.; Jamrozik, J. *J. Am. Chem. Soc.* **1990**, *112*, 1171.

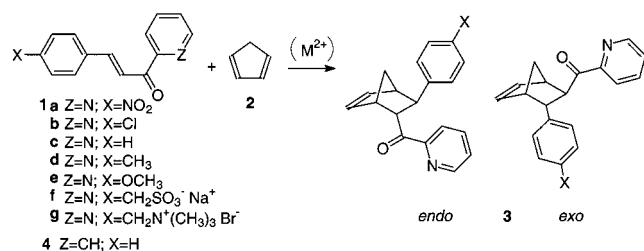
(20) Bunton, C. A. *Solution Chemistry of Surfactants*; Plenum Press: New York, 1979; p 519.

(21) Singh, V. K.; Raju, B. N. S.; Deota, P. T. *Synth. Commun.* **1988**, *18*, 567.

(22) (a) Jaeger, D. A.; Wang, J. *Tetrahedron Lett.* **1992**, *33*, 6415. (b) Jaeger, D. A.; Wang, J. *J. Org. Chem.* **1993**, *58*, 6745.

(23) Diego-Castro, M. J.; Hailes, H. C. *Tetrahedron Lett.* **1998**, *39*, 2211.

## Scheme 1



demonstrated that, compared to the reactions in pure water, the accelerations induced by micelles are generally modest<sup>7c,24</sup> and usually even retardations are observed.<sup>7g,25</sup> The inability of micelles to catalyze Diels–Alder reactions is surprising, since, in view of the nonpolar nature of most dienes and dienophiles, micellar catalysis is anticipated. In the present study, we will shed light on this discrepancy. As far as we know, we report herein the first detailed kinetic study of micellar catalysis of Diels–Alder reactions. It also represents the first in-depth study of Lewis acid catalysis in conjunction with micellar catalysis,<sup>26</sup> a combination that has recently found application in synthetic organic chemistry.<sup>27</sup>

## Results and Discussion

In previous studies, we described the Diels–Alder reaction between a class of bidentate dienophiles 3-(para-substituted phenyl)-1-(2-pyridyl)-2-propen-1-ones **1a–e** and cyclopentadiene (**2**) leading to racemic mixtures of endo as well as exo adducts **3** (Scheme 1).<sup>9</sup> Compounds **1** are relatively poor dienophiles, but once coordinated to a Co<sup>2+</sup>, Ni<sup>2+</sup>, Cu<sup>2+</sup>, or Zn<sup>2+</sup> cation, they react rapidly with **2** to give cycloadducts **3**.<sup>28</sup>

We describe the influence of micelles of CTAB, SDS, and dodecyl heptaoxyethylene ether (C<sub>12</sub>E<sub>7</sub>) as well as copper and zinc didodecyl sulfate (M(DS)<sub>2</sub>)<sup>29</sup> on the rates and selectivities of the uncatalyzed as well as the Lewis acid-catalyzed Diels–Alder reactions of **1** and **2**. Particularly the micelles bearing catalytically active transition-metal counterions are interesting, since they are likely to exhibit micellar catalysis and Lewis acid catalysis simultaneously.

Note that the dienophiles can be divided into nonionic (**1a–e**), anionic (**1f**), and cationic (**1g**) species. A comparison of the effects of nonionic (C<sub>12</sub>E<sub>7</sub>), anionic (SDS, Cu(DS)<sub>2</sub>), and cationic (CTAB) micelles on the rates of their reaction with **2** will allow assessment of the importance of electrostatic interactions in micellar catalysis.

(24) Wijnen, J. W.; Engberts, J. B. F. N. *Liebigs Ann./Recl.* **1997**, 1085.

(25) (a) Breslow, R.; Maitra, U.; Rideout, D. *Tetrahedron Lett.* **1983**, 24, 1901. (b) Sangwan, N. K.; Schneider, H. *J. Chem. Soc., Perkin Trans. 2* **1989**, 1223. (c) Hunt, I.; Johnson, C. D. *J. Chem. Soc., Perkin Trans. 2* **1991**, 1051.

(26) Alternatively, metallomicelles have been used extensively as catalysts for ester and amide hydrolysis reactions. However, in these processes, the metal ions do not act primarily as Lewis acids. For examples, see: (a) Tagaki Ogino, K.; Kashihara, N.; Ueda, T.; Isaka, T.; Yoshida, T.; Tagaki, W. *Bull. Chem. Soc. Jpn.* **1992**, 65, 373. (b) Scrimin, P.; Tecilla, P.; Tonellato, U. *J. Phys. Org. Chem.* **1992**, 5, 619. (c) Cleij, M. C.; Mancin, F.; Scrimin, P.; Tecilla, P.; Tonellato, U. *Tetrahedron* **1997**, 53, 357 and references therein.

(27) (a) Kobayashi, S.; Wakabayashi, T.; Oyamada, H. *Chem. Lett.* **1997**, 831. (b) Kobayashi, S.; Wakabayashi, T.; Nagayama, S.; Oyamada, H. *Tetrahedron Lett.* **1997**, 38, 4559.

(28) The presence of aromatic  $\alpha$ -amino acids can induce enantioselectivity of this reaction in water: Otto, S.; Boccaletti, G.; Engberts, J. B. F. *N. J. Am. Chem. Soc.* **1998**, 120, 4238.

(29) (a) Satake, I.; Iwamatsu, I.; Hosokawa, S.; Matuura, R. *Bull. Chem. Soc. Jpn.* **1963**, 36, 204. (b) Satake, I.; Matuura, R. *Bull. Chem. Soc. Jpn.* **1963**, 36, 813. (c) Moroi, Y.; Motomura, K.; Matuura, R. *J. Colloid Interface Sci.* **1974**, 46, 111. (d) Kamenka, N.; Burgaud, I.; Treiner, C.; Zana, R. *Langmuir* **1994**, 10, 3455.

**Table 1.** Influence of Micelles of CTAB, SDS, and C<sub>12</sub>E<sub>7</sub> on the Apparent Second-Order Rate Constants (M<sup>-1</sup> s<sup>-1</sup>)<sup>a</sup> for the Diels–Alder Reaction between **1a**, **1f**, and **1g**, respectively, and **2** at 25 °C<sup>b</sup>

medium <sup>c</sup>	<b>1a</b>	<b>1f</b>	<b>1g</b>
water	4.02 × 10 <sup>-3</sup>	1.74 × 10 <sup>-3</sup>	2.45 × 10 <sup>-3</sup>
SDS	3.65 × 10 <sup>-3</sup>	1.44 × 10 <sup>-3</sup>	1.47 × 10 <sup>-3</sup>
CTAB	3.61 × 10 <sup>-3</sup>	2.83 × 10 <sup>-4</sup>	2.01 × 10 <sup>-3</sup>
C <sub>12</sub> E <sub>7</sub>	3.35 × 10 <sup>-3</sup>	1.62 × 10 <sup>-3</sup>	2.05 × 10 <sup>-3</sup>

<sup>a</sup>  $k_{app} = k_{obs}/[2]_t$  wherein  $[2]_t$  is the overall concentration of **2**. <sup>b</sup>  $[1] \approx 2 \times 10^{-5}$  M;  $[2] = 2.0 \times 10^{-3}$  M. <sup>c</sup> All solutions contain 1.0 × 10<sup>-4</sup> M EDTA in order to suppress catalysis by trace amounts of transition metal ions. The concentration of surfactant is 7.8 mM above the cmc of the particular compound under the reaction conditions.

**Effects of Micelles on the Rate and Selectivity of the Uncatalyzed Diels–Alder Reaction.** The effect of micelles of SDS, CTAB, and C<sub>12</sub>E<sub>7</sub> on the apparent second-order rate constants ( $k_{app}$ ) of the Diels–Alder reaction between nonionic **1a**, anionic **1f**, and cationic **1g**, respectively, with **2** is summarized in Table 1. For all entries, the concentration of surfactant is 7.8 mM above the cmc of the particular amphiphile.<sup>30</sup> The rate constants have been obtained by following the decrease of the UV–visible absorbance of **1** by employing spectroscopic techniques. This technique allows the use of low concentrations of **1** ( $\sim 2 \times 10^{-5}$  M) so that, on average, there will be no more than one dienophile molecule per micelle. The overall concentration of **2** is 2.0 mM, which ensures that, depending on the aggregation number of the surfactant, the average number of cyclopentadiene molecules per micelle varies between 1 and 3.<sup>31</sup> Under these conditions, the effect of micelles on the rate of the Diels–Alder reaction is obviously small and invariably results in a slight *inhibition* of the reaction. It is striking to observe that the most significant effect occurs for anionic **1f** in CTAB solutions and for cationic **1g** in SDS solutions. These are the two combinations where one would expect essentially complete binding of the dienophile to the micelle as a result of favorable electrostatic interactions in addition to hydrophobic interactions. Apparently, reaction in the micellar environment is slower than that in the bulk aqueous phase, despite the anticipated increased concentrations of the reactants in the micellar pseudophase. Note that also in the case where electrostatic interactions inhibit binding of the dienophile to the micelle, i.e., **1f** in SDS and **1g** in CTAB solution, a retardation of the reaction is observed. In these cases, the dienophile most likely will reside primarily in the aqueous phase. Presumably, the retardation will then result from a decrease in the concentration of **2** in this phase due to its partial solubilization by the micelles.

To interpret the data in Table 1 in a quantitative fashion, we have analyzed the kinetics in terms of the pseudophase model (Figure 1). For the limiting cases of essentially complete binding of the dienophile to the micelle (**1f** in CTAB and **1g** in SDS solution) the following expression can be derived (see Supporting Information):

$$\frac{[2]_t}{k_{obs}} = \frac{V_{mol,S}}{k_m} [S] + \frac{V_w}{P_2 V_t k_m} + \frac{cmc V_{mol,S}}{k_m} \quad (1)$$

Herein  $[2]_t$  is the total number of moles of **2** present in the reaction mixture, divided by the total reaction volume  $V_t$ ;  $k_{obs}$

(30) For all ionic surfactants, the cmc has been determined under the Diels–Alder reaction conditions, which yielded values 3–14% lower than the cmc's of the surfactant in water.

(31) To estimate these values, we have used the partition coefficients of **2**, which will be derived later in this article.

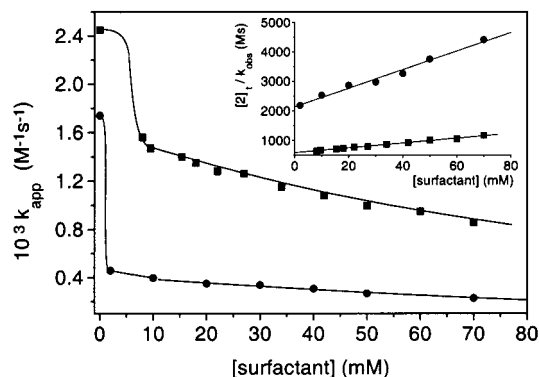


**Figure 2.** Apparent second-order rate constant,  $k_{app}$  ( $= k_{obs}/[2]_t$ ) versus the concentration of surfactant for the Diels–Alder reaction of **1f** with **2** in CTAB solution (●) and of **1g** with **2** in SDS solution (■) at 25 °C. The inset shows the treatment of these data using eq 1. From slopes and intercepts,  $P_2$  and  $k_m$  can be calculated (see Table 2).

**Table 2.** Analysis Using the Pseudophase Model<sup>a</sup>

surfactant	dienophile	$k_m$ ( $M^{-1} s^{-1}$ ) ( $\pm 10\%$ )	$P_2$ ( $\pm 10\%$ )
CTAB	<b>1f</b>	$5.9 \times 10^{-6}$	68
SDS	<b>1g</b>	$3.1 \times 10^{-5}$	61

<sup>a</sup> Partition coefficients for **2** over CTAB or SDS micelles and water and second-order rate constants for the Diels–Alder reaction of **1f** and **1g** with **2** in, respectively, the CTAB and SDS micellar pseudophase at 25 °C.

is the observed pseudo-first-order rate constant;  $V_{mol,S}$  is an estimate of the molar volume of micellized surfactant **S**;<sup>32</sup>  $k_m$  is the second-order rate constant in the micellar pseudophase (see Figure 1);  $V_w$  is the volume of the aqueous phase; and  $P_2$  is the partition coefficient of **2** over the micellar pseudophase and water. From the dependence of  $[2]_t/k_{obs}$  on the concentration of surfactant,  $P_2$  and  $k_m$  can be obtained. We have used estimates for the molar volume of micellized CTAB<sup>33</sup> and SDS<sup>34</sup> of 0.25 and 0.37  $M^{-1}$ , respectively, and assumed  $V_w/V_t = 1$ , which is reasonable in view of the low concentrations of surfactant used. Figure 2 shows the dependence of the apparent rate constants ( $k_{obs}/[2]_t$ ) on the concentration of surfactant for the Diels–Alder reactions of **1f** and **1g** with **2**. The results of the analysis in terms of the pseudophase model are shown in the inset in Figure 2 and in Table 2. The partition coefficients of **2** over SDS or CTAB micelles and water are similar. Comparison of the rate constants in the micellar pseudophase calculated by using the pseudophase model with those in water demonstrates a remarkable retardation induced by the micelles. This would suggest that the Diels–Alder reaction experiences an apolar medium, which is in contrast with previous reports that indicate waterlike environments for bimolecular micelle-catalyzed reactions.<sup>16e,19e,20</sup> Moreover, **1f** and **1g** contain ionic moieties, which makes it unlikely that they will be dragged deeply into the micelle.

The Diels–Alder reaction also provides us with a tool to probe its local reaction environment in the form of its endo/exo product ratio. A solvent polarity parameter has been based on endo/exo ratios of Diels–Alder reactions of methyl acrylate with cyclopentadiene.<sup>35</sup> Analogously we have determined the endo/exo ratio of the reaction between **1c** and **2** in surfactant

**Table 3.** Endo/Exo Product Ratios for the Diels–Alder Reaction of **1c** with **2** in Surfactant Solutions Compared to Water and Organic Solvents

medium	% endo/% exo ( $\pm 2\%$ )	medium	% endo/% exo ( $\pm 2\%$ )
100 mM CTAB	86/14	water	84/16 <sup>a</sup>
100 mM SDS	88/12	ethanol	77/23 <sup>a</sup>
100 mM $C_{12}E_7$	85/15	acetonitrile	67/33 <sup>a</sup>

<sup>a</sup> Data taken from ref 9b.

solution and in a number of different organic and aqueous media. These ratios are obtained from the <sup>1</sup>H NMR spectra of the product mixtures, as has been described previously.<sup>9b</sup> The results are summarized in Table 3 and clearly point toward a waterlike medium for the Diels–Alder reaction in the presence of micelles, which is in line with literature observations.<sup>36</sup> This seems definitely in conflict with the outcome of the analysis using the pseudophase model.

**Effects of Micelles on the Rate and Selectivity of the Lewis Acid-Catalyzed Diels–Alder Reaction.** In the previous section it was demonstrated that, in the absence of Lewis acid catalysts, micelles inhibit the Diels–Alder reaction between **1** and **2**, irrespective of the charge of the dienophile and the micelle. Since this Diels–Alder reaction can be catalyzed by transition-metal ions, we have also studied the effect of micelles on this process. The complexation behavior of **1** with transition-metal ions has been studied using UV–visible spectroscopy. Figure 3 shows the spectra of nonionic **1c** as well as the anionic and cationic counterparts **1f** and **1g** in water and in surfactant solutions containing copper(II) ions. The shifts of the absorption bands primarily reflect the extent of coordination of the dienophile to the copper ions. Binding to micelles has a negligible influence on the spectrum. Addition of  $C_{12}E_7$  to a 10 mM  $Cu(NO_3)_2$  solution containing the ionic dienophiles **1f** and **1g** leaves the absorption spectra essentially unchanged. Apparently **1f** and **1g** have little affinity for  $C_{12}E_7$  micelles. A similar picture emerges for cationic **1g**, which resides preferably in the aqueous phase rather than binding to cationic CTAB micelles. In contrast, **1c** has some affinity for  $C_{12}E_7$  and CTAB micelles, resulting in a decreased coordination to the copper ions in the presence of these surfactants. Interestingly, all three dienophiles, even anionic **1f**, bind more efficiently to the copper ions in the presence of  $Cu(DS)_2$  micelles than in aqueous solution containing twice the overall concentration of copper ions. This is in line with literature observations<sup>37</sup> that revealed an increased interaction between transition-metal ions and chelating organic molecules in the presence of anionic surfactant. The enhanced binding predicts a catalytic potential for these solutions and prompted us to investigate the influence of the different types of micelles on the rate of the copper ion-catalyzed reaction. Table 4 summarizes the results, which are in perfect agreement with the conclusions drawn from the complexation studies. In all surfactant solutions, **2** is expected to prefer the nonpolar micellar environment over the bulk aqueous phase. Consequently, those surfactant/dienophile combinations where the dienophile resides primarily in the aqueous phase show inhibition. This is the case for **1f** and **1g** in  $C_{12}E_7$  solution and for **1g** in CTAB solution. On the other hand, when diene, dienophile, and copper ion simultaneously bind to the micelle, as is the case for  $Cu(DS)_2$  solutions with all three dienophiles, efficient micellar catalysis is observed. An intermediate situ-

(32) Inevitably, the estimate of a molar volume of the micellized surfactant that is available for solubilization is somewhat arbitrary.

(33) Dearden, L. V.; Woolley, E. L. *J. Phys. Chem.* **1987**, *91*, 4123.

(34) De Lisi, R.; Liveri, T.; Castagnolo, M.; Inglesse, A. *J. Solution Chem.* **1986**, *15*, 23.

(35) Berson, J. A.; Hamlet, Z.; Mueller, W. A. *J. Am. Chem. Soc.* **1962**, *84*, 297.

(36) Braun, R.; Schuster, F.; Sauer, J. *Tetrahedron Lett.* **1986**, *27*, 1285.

(37) (a) James, A. D.; Robinson, B. H. *J. Chem. Soc., Faraday Trans. 1* **1977**, *73*, 10. (b) Robinson, B. H.; White, N. C. *J. Chem. Soc., Faraday Trans. 1* **1978**, *74*, 2625.

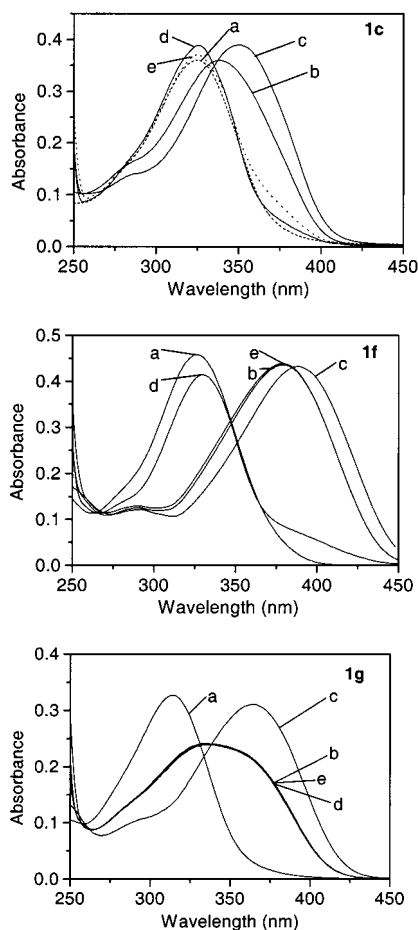


**Figure 3.** UV spectra of **1c**, **1f**, and **1g** in water (a) compared to those in solutions containing 10 mM  $\text{Cu}(\text{NO}_3)_2$  (b), 5 mM  $\text{Cu}(\text{DS})_2$  (c), 10 mM CTAB plus 10 mM  $\text{Cu}(\text{NO}_3)_2$  (d), and 10 mM  $\text{C}_{12}\text{E}_7$  plus 10 mM  $\text{Cu}(\text{NO}_3)_2$  (e).

**Table 4.** Influence of Micelles of  $\text{Cu}(\text{DS})_2$ , CTAB, and  $\text{C}_{12}\text{E}_7$  on the Apparent Second-Order Rate Constants ( $\text{M}^{-1} \text{s}^{-1}$ ) for the Copper(II)-Catalyzed Diels–Alder Reaction between **1c**, **1f**, and **1g**, Respectively, and **2** at 25 °C<sup>a</sup>

medium	<b>1c</b>	<b>1f</b>	<b>1g</b>
10 mM $\text{Cu}(\text{NO}_3)_2$	1.11	1.38	2.13
5 mM $\text{Cu}(\text{DS})_2$	5.95	5.50	15.3
CTAB <sup>b</sup> + 10 mM $\text{Cu}(\text{NO}_3)_2$	0.401	0.150	1.84
$\text{C}_{12}\text{E}_7$ <sup>b</sup> + 10 mM $\text{Cu}(\text{NO}_3)_2$	0.630	1.08	1.71

<sup>a</sup>  $[\mathbf{1}] \approx 2 \times 10^{-5} \text{ M}$ ;  $[\mathbf{2}] = 1.0 \times 10^{-3} \text{ M}$ . <sup>b</sup> The concentration of surfactant is 7.8 mM above the cmc of the particular compound under reaction conditions.

ation exists for **1c** in CTAB or  $\text{C}_{12}\text{E}_7$  solutions and particularly for **1f** in CTAB solution. Now the dienophile binds to the micelle and is shielded from the copper ions that apparently prefer to reside in the aqueous phase. This results in an overall retardation, despite the possible locally increased concentration of **2** in the micelle.

Very promising catalytic results were obtained for the  $\text{Cu}(\text{DS})_2$  solutions. We have analyzed this system in some detail. Figure 4 shows the dependence of the rate of the Diels–Alder reaction between **1c**, **1f**, and **1g**, respectively, with **2** on the concentration of  $\text{Cu}(\text{DS})_2$ . For all three dienophiles, the apparent second-order rate constant for their reaction with **2** increases dramatically when the concentration of  $\text{Cu}(\text{DS})_2$  reaches the cmc (1.11 mM). Beyond the cmc, the behavior of the rate at increasing surfactant concentration is subject to two counteractive influences. First, at higher surfactant concentra-

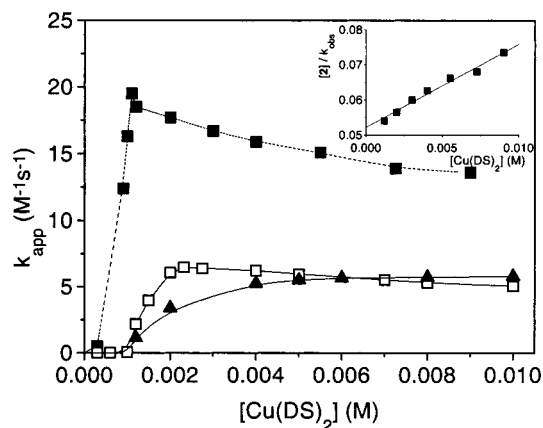


**Figure 4.** Apparent second-order rate constant ( $k_{\text{app}}$ ) versus the concentration of  $\text{Cu}(\text{DS})_2$  for the Diels–Alder reaction of **1c** ( $\square$ ), **1f** ( $\blacktriangle$ ) and **1g** ( $\blacksquare$ ) with **2** at 25 °C. The inset shows the treatment of the data for the reaction of **1g** according to the pseudophase model.

tion, a larger fraction of dienophile will be bound to the micelle, where it reacts faster than in bulk water, resulting in an increase in the rate of the reaction. Second, at the same time, the concentration of diene bound to the micelle will drop with increasing number of micelles, resulting in a decrease of the apparent second-order rate constant. At higher surfactant concentrations, the dienophile will be nearly completely bound to the micelles and the dilution effect will dominate the behavior. Together, these two effects result in the appearance of a rate maximum at a specific concentration of surfactant that is typical for micelle-catalyzed bimolecular reactions.<sup>16</sup> The position of the maximum depends primarily on the micelle–water partition coefficient of the dienophile. For instance, cationic **1g** reacts fastest close to the cmc, because of its very high affinity for the anionic  $\text{Cu}(\text{DS})_2$  micelles. Formation of a complex with a copper cation will only increase the affinity for the micelles. As a result, **1g** will be almost completely bound to the micelles, even at very low concentrations of  $\text{Cu}(\text{DS})_2$ . By contrast, the reaction of **1f** still benefits from an increasing surfactant concentration at 10 mM  $\text{Cu}(\text{DS})_2$ . In fact, it is surprising that the Diels–Alder reaction of this anionic compound is catalyzed at all by an anionic surfactant. Probably it is the copper complex of **1f**, being overall cationic, that binds to the micelle. Not surprisingly, the neutral **1c** shows intermediate behavior.

Interestingly, at very low concentrations of micellized  $\text{Cu}(\text{DS})_2$ , the rate of the reaction of **1a** with **2** was observed to be zero order in **1a** and dependent only on the concentration of  $\text{Cu}(\text{DS})_2$  and **2**. This is similar to the turnover and saturation kinetics exhibited by enzymes. The acceleration, relative to the reaction in organic media in the absence of catalyst, also approaches enzyme-like magnitudes: compared to the reaction in acetonitrile,  $\text{Cu}(\text{DS})_2$  micelles accelerate the Diels–Alder reaction between **1a** and **2** by a factor of 1 800 000.<sup>38</sup> This uncommonly high catalytic efficiency shows how a combination of a beneficial aqueous solvent effect, Lewis acid catalysis, and micellar catalysis can lead to extremely large accelerations.

The essentially complete binding of **1g** to the  $\text{Cu}(\text{DS})_2$  micelles allows treatment of the kinetic data shown in Figure 4 using the pseudophase model. Since it is likely that **1g** binds in the Stern region (vide infra), complete binding to the copper ions can be assumed. Using eq 1, the  $\text{Cu}(\text{DS})_2$ –water distribution coefficient of **2** can now be obtained as well as the second-order rate constant for the reaction in the micellar pseudophase

(38) Rate constant in acetonitrile,  $1.40 \times 10^{-5} \text{ M}^{-1} \text{ s}^{-1}$ ; rate constant in 2.4 mM  $\text{Cu}(\text{DS})_2$  solution,  $25.1 \text{ M}^{-1} \text{ s}^{-1}$ .

**Table 5.** Hammett  $\rho$ -Values for the Copper(II)-Catalyzed Diels–Alder Reaction between **1a–e** and **2** in Different Media

medium	$\rho$
10 mM Cu(DS) <sub>2</sub>	0.86
10 mM Cu(NO <sub>3</sub> ) <sub>2</sub> in acetonitrile	0.96 <sup>b</sup>
10 mM Cu(NO <sub>3</sub> ) <sub>2</sub> in ethanol	1.00 <sup>b</sup>
10 mM Cu(NO <sub>3</sub> ) <sub>2</sub> in water <sup>a</sup>	0.82 <sup>b</sup>

<sup>a</sup> Ionic strength 2.00 M (KNO<sub>3</sub>). <sup>b</sup> Data taken from ref 9b.

(see inset in Figure 4). Unfortunately no literature data exist for the molar volume of micellized Cu(DS)<sub>2</sub> that is required for the kinetic analysis. We have used an estimate of 0.50 M<sup>-1</sup>, twice as large as the number that we have used previously for micellized SDS.<sup>39</sup> Calculations using this value yield a partition coefficient for **2** of 96 and a micellar second-order rate constant of 0.21 M<sup>-1</sup> s<sup>-1</sup>. This partition coefficient is higher than the corresponding values for SDS and CTAB micelles given in Table 2. This is in agreement with literature data, that indicate that Cu(DS)<sub>2</sub> micelles are able to solubilize 1.5 times as much benzene as SDS micelles.<sup>29b</sup> Most likely this is a result of the higher counterion binding of Cu(DS)<sub>2</sub> micelles (89 versus 60%), which reduces the headgroup repulsion and allows a tighter packing of the headgroups resulting in decreased water penetration and an increased nonpolar character of the micellar binding sites compared to SDS. Comparing the value of the micellar second-order rate constant of 0.21 M<sup>-1</sup> s<sup>-1</sup> with the rate constants for the reaction in acetonitrile (0.472 M<sup>-1</sup> s<sup>-1</sup>) and ethanol (0.309 M<sup>-1</sup> s<sup>-1</sup>) again suggests an apolar reaction medium for the Diels–Alder reaction. This is hard to reconcile with the ionic character of two of the three reaction partners involved. To obtain more insight into the local environment of the catalyzed reaction, we have investigated the influence of substituents on the rate constants for this process in micellar solution and compared it to the corresponding effect in different aqueous and organic solvents. Plots of the logarithms of the rate constants versus the Hammett  $\sigma$ -values show good linear dependences for all media. The resulting  $\rho$ -values are shown in Table 5. The  $\rho$ -value in Cu(DS)<sub>2</sub> solution resembles that in aqueous solution more than those in organic solvents. Therefore, it appears that the outcome of the analysis using the pseudophase model is not in agreement with experimental observations. Apparently, one (or more) of the assumptions of the pseudophase model is not valid for the system studied here. In particular, the treatment of the micellar pseudophase as a homogeneous “solution” might not be warranted. Therefore, we contend that diene and dienophile, on average, reside in different parts of the micelle, thereby impeding the reaction. This would also explain the absence of a large catalytic effect in cases where diene and dienophile bind efficiently to the micelle. To check this hypothesis, we have probed the binding location of diene and dienophile using <sup>1</sup>H NMR techniques.

**Binding Locations of Diene and Dienophile and Their Implications.** NMR methods have been regularly employed in the study of micellar solutions.<sup>40</sup> The most frequently encountered technique to probe the binding location of aromatic compounds in micelles makes use of changes in the chemical shifts in the <sup>1</sup>H NMR spectrum of the surfactant that are induced by the aromatic ring of the solubilize.<sup>11a,j,41</sup> Such studies with a large number of aromatic compounds have revealed that for CTAB the largest shift occurs for the alkyl chain protons near

(39) The number for the molar volume of micellized Cu(DS)<sub>2</sub> is probably too large. Using a smaller number will result in a larger value for  $P_2$  and a decrease of  $k_m$  which will even further justify the conclusions drawn from these numbers.

(40) Chachaty, C. *Prog. NMR Spectrosc.* **1987**, *19*, 183.

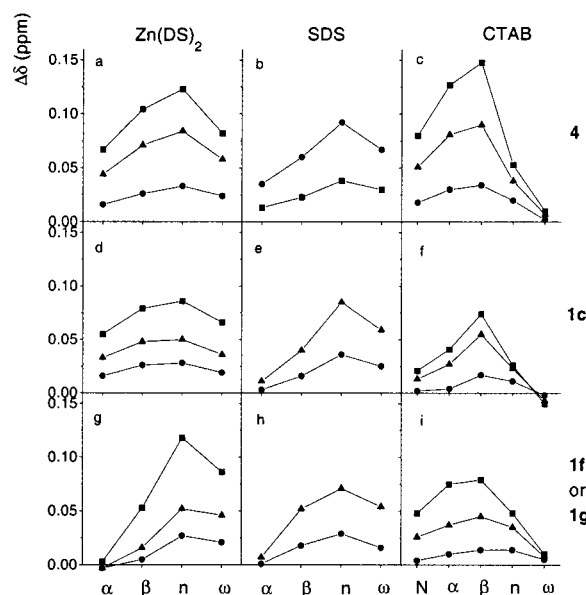


**Figure 5.** Aromatic solubilize-induced changes in the chemical shift of the proton NMR signals of micellized surfactant. (a–f) show the effect of **4** and **1c** on the proton resonances of Zn(DS)<sub>2</sub> (25 mM), SDS (50 mM), and CTAB (50 mM). (g) and (h) show the corresponding effect of **1g** on Zn(DS)<sub>2</sub> (25 mM) and SDS (50 mM), respectively. (i) depicts the effect of **1f** on the CTAB (50 mM) resonances. The concentrations of the solubilize were 2.0 (●), 5.0 (▲) or 8 (■) mM. N stands for the protons at the three headgroup methyl moieties of CTAB,  $\alpha$  and  $\beta$  stand for the methylene protons at the  $\alpha$  and  $\beta$  positions relative to the headgroup.  $\omega$  represents the terminal methyl group protons and  $n$  the protons between the  $\beta$ - and  $\omega$ -positions.

the surfactant headgroup, whereas in SDS nearly all proton signals are shifted significantly, but with the most pronounced shifts for the protons around the center of the chain. This has been interpreted in terms of a deeper penetration of aromatic compounds in SDS micelles relative to CTAB micelles.<sup>41b,e,g</sup>

We have determined the aromatic shifts that are induced by **1c**, **1f**, and **1g** in the <sup>1</sup>H NMR spectra of SDS, CTAB, and Zn(DS)<sub>2</sub>. The latter is used as a model system for Cu(DS)<sub>2</sub>, which is paramagnetic. The cmc's and counterion binding of Cu(DS)<sub>2</sub> and Zn(DS)<sub>2</sub> are very similar,<sup>29a</sup> and Zn(II) ions have been reported to be also capable of coordinating to **1**, albeit somewhat less efficiently than copper ions.<sup>9b</sup> Figure 5 shows the results of the chemical shift measurements. For the purpose of comparison the data for chalcone (**4**) have been added. This compound has almost no tendency to coordinate to transition-metal ions in aqueous solutions.<sup>9b</sup> In Figure 5 and throughout the rest of this study, N stands for the protons at the three headgroup methyl moieties of CTAB;  $\alpha$  and  $\beta$  stand for the methylene protons at the  $\alpha$ - and  $\beta$ -positions relative to the headgroup of the surfactant.  $\omega$  represents the terminal methyl group protons and  $n$  the protons between the  $\beta$ - and  $\omega$ -positions.

From the data in Figure 5, a number of conclusions can be drawn. (1) The shifts induced by **1c** on the NMR signals of SDS and CTAB show the characteristics usually observed for benzene derivatives.<sup>11a,j,41</sup> (2) Introduction of an ionic group into the dienophile (compare panel e of Figure 5 with (h) and

(41) (a) Tokiwa, F.; Tsujii, K. *J. Phys. Chem.* **1971**, *75*, 3560. (b) Fendler, E. J.; Day, C. L.; Fendler, J. H. *J. Phys. Chem.* **1972**, *76*, 1460. (c) Ganesh, K. N.; Mitra, P.; Balasubramanian, D. *J. Phys. Chem.* **1982**, *86*, 4291. (d) Bunton, C. A.; Cowell, C. P. *J. Colloid Interface Sci.* **1988**, *122*, 154. (e) Fornasiero, D.; Grieser, F.; Sawyer, W. H. *J. Phys. Chem.* **1988**, *92*, 2301. (f) Gao, Z. Ph.D. Thesis, Dalhousy University, Halifax, 1989. (g) Wasylshen, R. E.; Kwak, J. C. T.; Gao, Z.; Verpoorte, E.; MacDonald, J. B.; Dickson, R. M. *Can. J. Chem.* **1991**, *69*, 822.

(f) with (i)) causes this compound to bind more closely to the headgroups of the micelles. (3) Chelation of the dienophile to a zinc(II) ion has little effect on its location in the micelle (compare (a) with (d)). (4) The presence of the pyridine nitrogen atom influences the binding location only to a minor extent (compare (b) with (e) and (c) with (f)). Surprisingly, the shifts observed in the  $^1\text{H}$  NMR spectrum of  $\text{Zn}(\text{DS})_2$  as caused by **1g** seem to point toward a relatively deep penetration of this compound into the micelle. This is extremely unlikely. **1g**, when bound to  $\text{Zn}(\text{DS})_2$  micelles, will coordinate to a Zn(II) ion. The resulting complex will now have three positive charges: two of the zinc ion at one end of the complex and one of the trimethylammonium group at the other end. It is hard to imagine that this hydrophilic complex will penetrate into the nonpolar core of the micelle. Still the shifts indicate a short distance between the *n* protons of the surfactant and the aromatic rings of **1g**. A likely explanation for this behavior is bending of the alkyl chain of the surfactant toward the aromatic parts of the dienophile. This demonstrates that an interpretation of shift data solely in terms of depth of penetration into the micelle is hazardous. The observed shifts of surfactant protons merely indicate a proximity of aromatic groups and, strictly, do not provide direct information about the location where this encounter takes place. Still, we suggest that we may draw at least one solid conclusion from the data in Figure 5: on average, the dienophile is not in the core of the micelle.

In a second attempt to obtain more insight into the binding location of the dienophile and now also of the diene, we have employed the well-documented influence of paramagnetic ions on the spin–lattice relaxation rates of species in their proximity.<sup>42</sup> The spin–lattice relaxation rate is dramatically enhanced close to these ions. This effect is highly distance-dependent. Such paramagnetic relaxation techniques have found application in surfactant chemistry.<sup>41g,43</sup> Generally, one can select the charge of the paramagnetic ion so that it will act as a counterion of the micellar system under study, which ensures that it will be located primarily in the Stern region of the micelle. Consequently, compounds bound to the outer regions of the micelle will experience a much larger influence of these paramagnetic ions than compounds located in the interior of the micelle.<sup>41g</sup> The change in the relaxation rate induced by the paramagnetic ion ( $r_p$ ) can be assessed by subtracting the observed relaxation rates in the absence of these ions from those obtained in the presence of the paramagnetic species. The exact magnitude of  $r_p$  is strongly dependent upon the local concentration of the paramagnetic ions at the micelle. Consequently, normalization of the  $r_p$  values is required before comparisons between separately prepared solutions can be made. Hence, throughout this study, the  $r_p$  values will be expressed as a percentage of the  $r_p$  value of the methylene group next to the surfactant headgroup.

We have used the paramagnetic relaxation technique to study the binding locations of **1c**, **1f**, or **1g** and **2** in CTAB, SDS or  $\text{Zn}(\text{DS})_2$  solutions by employing  $[\text{Cu}(\text{EDTA})]^{2-}$ ,  $\text{Cu}^{2+}$  (for **2**), or  $\text{Dy}^{3+}$  (for **1**) as paramagnetic species. Figure 6 shows the

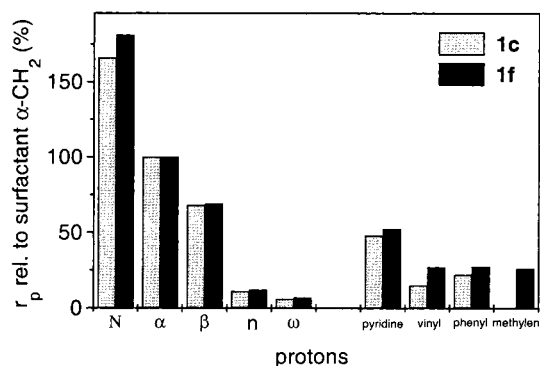


**Figure 6.** Paramagnetic ion-induced spin–lattice relaxation rates ( $r_p$ ) of the protons of **1c** and **1f** in CTAB solution and of CTAB in the presence of **1c** or **1f**, normalized to  $r_p$  for the surfactant  $\alpha\text{-CH}_2$ . The solutions contained 50 mM CTAB, 8 mM **1c** or **1f**, and 0 or 0.4 mM  $[\text{Cu}(\text{EDTA})]^{2-}$ .

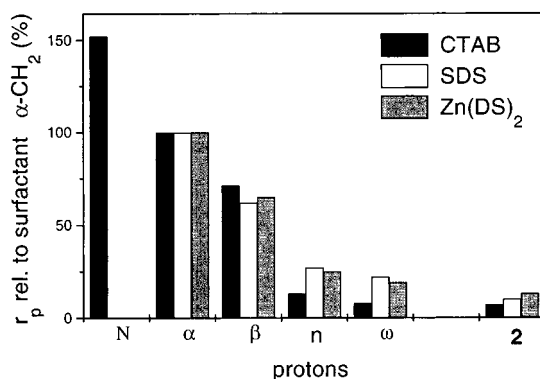


**Figure 7.** Paramagnetic ion-induced spin–lattice relaxation rates ( $r_p$ ) of the  $\text{CH}_2$  protons of **2** in CTAB, SDS, or  $\text{Zn}(\text{DS})_2$  solution and of these surfactants in the presence of **2**, normalized to  $r_p$  for the surfactant  $\alpha\text{-CH}_2$ . The solutions contained 25 mM  $\text{Zn}(\text{DS})_2$ , 50 mM CTAB or SDS, 3 mM **2** and 0 or 0.4 mM  $[\text{Cu}(\text{EDTA})]^{2-}$  for CTAB solutions, and 0 or 0.2 mM  $\text{Cu}^{2+}$  for SDS and  $\text{Zn}(\text{DS})_2$  solutions.

values of  $r_p$  relative to  $r_p$  of the surfactant  $\alpha$ -methylene protons for **1c** and **1f** in CTAB solution. To provide a frame of reference, the relative paramagnetic relaxation rates of the CTAB protons are also shown. The latter show a clear decrease upon going from the headgroup toward the end of the hydrocarbon chain. The values for both dienophiles are of a magnitude somewhere between those of the  $\beta$  and the *n* methylene protons of CTAB. Consequently, on average they are somewhat further away from the paramagnetic ions than the  $\beta$ -protons but not as far as the *n* protons.

The introduction of an ionic group (compare **1f** with **1c**) results in a modest decrease of the average distance to the paramagnetic ion. Presumably, two counteracting effects are operative. The presence of a charged group might well result in a shift of the average binding location toward the outer regions of the micelle, resulting in an increased influence of the paramagnetic ion on the rate of relaxation. On the other hand, the electrostatic repulsion between the charged substituent and the paramagnetic counterion will result in a decrease of the effect of this ion on the relaxation rate. Analogous studies on **1c** and **1g** in SDS and  $\text{Zn}(\text{DS})_2$  led to essentially the same conclusions and are not shown here.

Figure 7 visualizes the effect of paramagnetic ions on the relaxation rate of **2** in CTAB, SDS, and  $\text{Zn}(\text{DS})_2$  solutions.<sup>44</sup>

(44) **2** is molecularly dispersed up to concentrations of 0.04 M. (Blözkijl, W. Ph.D. Thesis, Groningen, 1991, p 136.) The concentrations of **2** used were well below this limit.

(42) Martin, M. L.; Delpuech, J. J.; Martin, G. J. *Practical NMR Spectroscopy*; Heyden: London, 1980.

(43) (a) Fox, K. K.; Robb, I. D.; Smith, R. J. *Chem. Soc., Faraday Trans. 1* **1972**, 68, 445. (b) van Bockstaele, M.; Gelan, J.; Martens, H.; Put, J.; de Schryver, F. C.; Dederen, J. C. *Chem. Phys. Lett.* **1980**, 70, 605. (c) Cabane, B. *J. Phys.* **1981**, 42, 847. (d) Zemb, T.; Chachaty, C. *Chem. Phys. Lett.* **1982**, 88, 68. (e) Chevalier, Y.; Chachaty, C. *J. Phys. Chem.* **1985**, 89, 875. (f) Chevalier, Y.; Chachaty, C. *J. Am. Chem. Soc.* **1985**, 107, 1102. (g) Jangannathan, N. R.; Venkateswaran, K.; Herring, F. G.; Patey, G. N.; Walker, D. C. *J. Phys. Chem.* **1987**, 91, 4553. (h) Gao, Z.; Wasylishen, R. E.; Kwak, J. C. T. *J. Phys. Chem.* **1989**, 93, 2190. (i) Gao, Z.; Wasylishen, R. E.; Kwak, J. C. T. *J. Chem. Soc., Faraday Trans.* **1991**, 87, 947.

**Table 6.** Effect of the Solubilize on the Paramagnetic Ion-Induced Spin–Lattice Relaxation Rates ( $r_p$ ) of the Protons of CTAB (C), SDS (S), and Zn(DS)<sub>2</sub> (Z), Normalized to  $r_p$  of the Surfactant  $\alpha$ -CH<sub>2</sub><sup>a,b</sup>

solubilize	N			$\alpha$			$\beta$			n			$\omega$		
	C	S	Z	C	S	Z	C	S	Z	C	S	Z	C	S	Z
	153	100	100	100	64	37	48	13	11	14	9	7	9		
<b>1c</b>	166	100	100	100	68	50		11	15		6	8			
<b>1f</b> or <b>1g</b> <sup>c</sup>	181	100	100	100	69	36	44	12	17	13	7	9	9		
<b>2</b>	152	100	100	100	71	62	65	13	27	25	8	22	19		

<sup>a</sup> For a definition of  $\alpha$ ,  $\beta$ ,  $n$ , and  $\omega$ , see Figure 5. <sup>b</sup> The solutions contained 25 mM Zn(DS)<sub>2</sub>, 50 mM CTAB or SDS, 3 mM **2** and 8 mM **1c**, **1f**, or **1g** and 0 or 0.4 mM [Cu(EDTA)]<sup>2-</sup> for CTAB solutions, and 0 or 0.2 mM Cu<sup>2+</sup> (with **2** as solubilize) or Dy<sup>3+</sup> (with **1** as solubilize) for SDS and Zn(DS)<sub>2</sub> solutions. <sup>c</sup> **1f** was used in CTAB solutions, whereas **1g** was used in SDS and Zn(DS)<sub>2</sub> solutions.

In this case, the relative value of  $r_p$  is invariably *smaller* than the corresponding effect on the  $\omega$ -methyl protons of the surfactant. This clearly demonstrates that diene **2**, in contrast to the dienophiles, is located in the interior of the micelle and does spend little time at the surface.

Careful analysis of the influence of the character of the solubilize on the relaxation data of the surfactant led to another interesting observation. Table 6 summarizes these data. The first row represents the relative  $r_p$  values of the different surfactant protons in the absence of any solubilize. The second and third rows show the corresponding effects in the presence of 8 mM **1c**, **1f**, or **1g**. The introduction of these compounds into a micellar solution does not lead to a significant perturbation of the alkyl chains of the micelle since the relative paramagnetic relaxation rates are similar to the those for the pure surfactant. Yet, when **2** is added to the solutions of SDS and Zn(DS)<sub>2</sub>, significant increases in the relative paramagnetic relaxation rates of the  $\beta$ -, the  $n$ -, and the  $\omega$ -protons are observed. Apparently, the nonpolar solute bound in the interior of these micelles pushes the alkyl chains of the individual surfactant molecules toward the surface. Curiously, this effect is completely absent for CTAB. This might be a result of the increased length of the alkyl chain of this surfactant compared to the two anionics, ensuring an increased tolerance toward incorporation of a solubilize.

In summary, the NMR studies indicate different average binding locations for diene and dienophile. The diene resides preferentially in the interior of the micelles, which is not surprising in view of its nonpolar character. The dienophiles, on the other hand, are located more toward the surface of the aggregates. This behavior has important implications for the rationalization of the kinetic data. Clearly, when the Diels–Alder reactants are not homogeneously distributed over the micellar pseudophase, analysis according to the pseudophase model will provide erroneous results. It will predict a second-order rate constant in the micellar pseudophase that is too low. However, the partition coefficients that are produced using this model are still correct, considering that they represent the ratio of the *average* concentrations of solubilize in the micellar phase and in the aqueous phase. Another consequence of the above analysis is that the surprising inefficiency of micellar aggregates to catalyze Diels–Alder reactions in the absence of Lewis acids can now be rationalized. Obviously, micelles are able to bind diene and dienophile efficiently *but at different locations in the micelle*. The reactions seem to take place at the surface of the micelle in a rather aqueous environment, where the concentration of diene is low. Therefore, inhibition most likely results from a local concentration effect rather than from a kinetic medium effect.

The only micellar system that shows efficient catalytic behavior is Cu(DS)<sub>2</sub>. These micelles concentrate both dienophile and copper ion at their surface, thereby promoting complexation of these compounds. Note that, at concentrations slightly higher than the cmc of Cu(DS)<sub>2</sub>, already very efficient coordination of the dienophile to copper can take place, which, in the absence of the surfactant, requires copper ion concentrations that are orders of magnitude higher.

Interestingly, the apparent rate constants obtained for the reaction between **1** with **2** in the presence of Cu(DS)<sub>2</sub> exceed those obtained in the case of complete binding of **1** to copper(II) ions in water. Apparently, the local concentration of **2** at the surface of the Cu(DS)<sub>2</sub> micelles is high enough to allow this rate enhancement. In contrast, at the surface of the SDS and CTAB, the concentration of **2** is lower as a result of the reduced partition coefficients of **2** for these micelles as compared to Cu(DS)<sub>2</sub>.

The results described in this article may well provide a rationale for the surprising inability of micelles to catalyze Diels–Alder reactions as is apparent from the literature. In view of the structures of most dienes and dienophiles, differences in the preferred location of binding of the reaction partners are expected, which will diminish the rate of their reaction.

## Conclusions

The Diels–Alder reaction of 3-(para-substituted phenyl)-1-(2-pyridyl)-2-propen-1-ones **1a–g**, containing neutral, cationic, or anionic substituents, and cyclopentadiene (**2**) in the absence of Lewis acids is retarded by micelles of CTAB, SDS, and C<sub>12</sub>E<sub>7</sub>. In the situation where the dienophile does not bind to the micelle, the reaction is inhibited because uptake of **2** in the micelles lowers its concentration in the aqueous phase. However, retardations are most pronounced when there is essentially complete binding of the dienophile to the micelle. In this case, the reaction still experiences a waterlike environment. We contend that the retardation mainly results from a significant difference in the binding locations of **1** and **2**, with the dienophiles preferring the outer regions of the micelle and the diene residing in the interior. Evidence comes from solubilize-induced aromatic shifts in the <sup>1</sup>H NMR spectra of the surfactants as well as from paramagnetic ion-induced relaxation enhancements of the <sup>1</sup>H NMR signals of the solubilize. The latter experiments also show that **2**, in contrast to **1**, perturbs the micelles of SDS and Cu(DS)<sub>2</sub>. Under conditions of inhomogeneous distribution of **1** and **2** over the micelle, kinetic analysis using the pseudophase model, which is so successful for many other micelle-catalyzed processes, leads to erroneous estimates of the second-order rate constant in the micellar pseudophase.

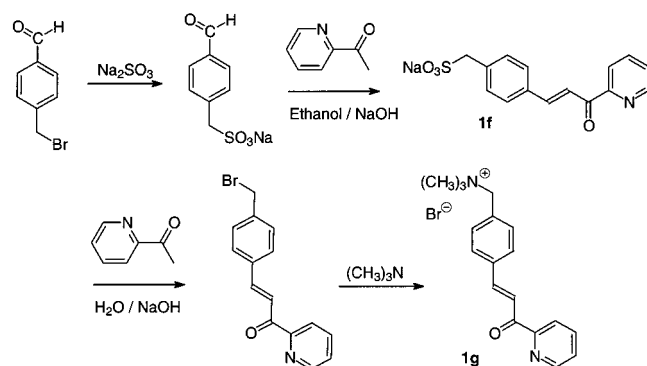
Micelles of Cu(DS)<sub>2</sub> induce rate enhancements up to a factor  $1.8 \times 10^6$  compared to the uncatalyzed reaction in acetonitrile. These enzyme-like accelerations result from efficient complexation of the dienophile to the catalytically active copper ions, both species being concentrated at the micellar surface. Moreover, the higher affinity of **2** for Cu(DS)<sub>2</sub> compared to SDS and CTAB micelles ( $P_2 = 96$  versus 61 and 68, respectively) will diminish the inhibitory effect due to spatial separation of **1** and **2** as observed for SDS and CTAB.

## Experimental Section

**Materials.** *trans*-Chalcone (**4**) (mp 57.1–57.7 °C) was obtained from Aldrich and crystallized from ethanol. Cyclopentadiene (**2**) was prepared from its dimer (Merck-Schuchardt) immediately before use. Dimineralized water was distilled twice in a quartz distillation unit. Cu(NO<sub>3</sub>)<sub>2</sub>·3H<sub>2</sub>O (Merck), KNO<sub>3</sub> (Merck), CTAB (Merck), SDS (BDH



## Scheme 2



Chemicals),  $C_{12}E_7$  (Nikko) and ethylenediaminetetraacetic acid tetrasodium salt trihydrate (EDTA, Aldrich) were of the highest purity available.  $Cu(DS)_2$  and  $Zn(DS)_2$  were prepared following literature procedures<sup>29c</sup> and were crystallized from water. Compounds **1a–e** were prepared by an aldol condensation of the corresponding substituted aldehyde with 2-acetylpyridine as has been described previously.<sup>9b</sup>  $^1H$  NMR shift and relaxation time measurements were performed in  $D_2O$  (99.9% D, Aldrich). Stock solutions of **1c** and **4** used in the NMR experiments were prepared in methanol- $d_4$  (99.8% D, CIL).

**1f** and **1g** were prepared as outlined in Scheme 2. Yields were not optimized. *p*-(Bromomethyl)benzaldehyde was prepared by reaction of *p*-(bromomethyl)benzotrionitrile (Acros) with diisobutylaluminum hydride following a literature procedure.<sup>45</sup>

**Sodium (*p*-Oxomethylphenyl)methyl Sulfonate.** A suspension of 3.90 g (19.6 mmol) of *p*-(bromomethyl)benzaldehyde and 4.00 g (31.7 mmol) of sodium sulfite in 40 mL of water was refluxed for 2 h, after which a clear solution was obtained. The reaction mixture was cooled in an ice bath, resulting in precipitation of some sodium sulfite. After filtration, the solvent was evaporated. Ethanol was added to the remaining solid, and the suspension was refluxed for 10 min. After filtering the hot solution, the filtrate was allowed to cool slowly to  $-18$  °C whereupon sodium (*p*-oxomethylphenyl)methyl sulfonate separated as colorless crystals. The extraction procedure was repeated two more times, affording 2.29 g (10.3 mmol, 53%) of the desired product:  $^1H$  NMR (200 MHz,  $D_2O$ )  $\delta$  (ppm) 4.10 (s, 2H), 7.44 (d, 2H), 7.76 (d, 2H), 9.75 (s, 1H).

**1f.** A solution of 75 mL of ethanol and 3.75 mL of a 10% solution of sodium hydroxide in water was cooled to 0 °C, and 2.13 g (9.57 mmol) of sodium (*p*-oxomethylphenyl)methyl sulfonate and 1.28 g (10.6 mmol) of 2-acetylpyridine were added. The solution was stirred for 16 h at 0 °C, and filtered affording 2.47 g (7.66 mmol, 80%) of crude **1f**. Crystallization from methanol yielded 1.08 g (35%) of the desired product: mp 220 °C (dec),  $^1H$  NMR (200 MHz,  $D_2O$ )  $\delta$  (ppm) 4.00 (s, 2H), 7.36 (d, 2H), 7.55 (m, 1H), 7.58 (d, 2H), 7.61 (m, 2H), 7.81 (m, 2H), 8.43 (d, 1H). Anal. Calcd for  $C_{15}H_{12}NO_4SNa$ : C, 55.4; H, 3.72; N, 4.31; S, 9.84; Na, 7.07. Found: C, 54.7;<sup>46</sup> H, 3.74; N, 4.19; S, 9.41; Na, 6.97.

**3-(*p*-Bromomethylphenyl)-1-(2-pyridyl)-2-propen-1-one.** A solution of 10 g of sodium hydroxide in 1000 mL of water was cooled to 0–5 °C. 2-Acetylpyridine (5.95 g, 49.2 mmol) and a solution of 7.25 g (36.4 mmol) *p*-(bromomethyl)benzaldehyde dissolved in a minimal amount of ethanol were added. The resulting suspension was stirred for 48 h at 0–5 °C. The product was filtered and washed extensively with water until the smell of the 2-acetylpyridine had disappeared. After drying at 50 °C under vacuum, 10.5 g (34.8 mmol, 96%) of 3-(*p*-(bromomethyl)phenyl)-1-(2-pyridyl)-2-propen-1-one was obtained:  $^1H$  NMR (200 MHz,  $CDCl_3$ )  $\delta$  (ppm) 4.50 (s, 2H), 7.42 (d,

2H), 7.44 (m, 1H), 7.70 (d, 2H), 7.85 (m, 1H), 7.91 (d, 1H), 8.20 (d, 1H), 8.31 (d, 1H), 8.75 (d, 1H).

**1g.** 3-(*p*-Bromomethylphenyl)-1-(2-pyridyl)-2-propen-1-one (5.00 g, 16.6 mmol) was suspended in 350 mL of anhydrous ether under a nitrogen atmosphere. A 20-mL aliquot of a 4.2 M solution of trimethylamine in ethanol (Fluka) was added. The reaction mixture was stirred for 24 h at room temperature under a nitrogen atmosphere. Evaporation of the solvents and excess of trimethylamine afforded crude **1g** in quantitative yield. The very hygroscopic product was crystallized from dry 1-propanol. Removal of this solvent from the crystals is not possible by conventional methods. However, dissolving the product in water, filtration, and subsequent freeze-drying afforded 3.10 g (8.59 mmol, 52%) of **1g**: mp 212.5 °C (dec);  $^1H$  NMR (200 MHz,  $CDCl_3$ )  $\delta$  (ppm) 3.44 (s, 9H), 5.16 (s, 2H), 7.50 (m, 1H), 7.75 (s, 4H), 7.84 (d, 1H), 7.85 (m, 1H), 8.01 (d, 1H), 8.31 (d, 1H), 8.72 (d, 1H). Anal. Calcd for  $C_{18}H_{21}BrN_2O$ : C, 60.0; H, 5.88; Br, 21.92; N, 7.78. Found: C, 59.8; H, 5.97; Br, 21.77; N, 7.58.

**Endo/Exo Ratios.** Endo/exo ratios of the micelle-catalyzed reactions were determined by adding 0.25 mmol of **1c** and 0.5 mmol of **2** to a solution of 5 mmol of surfactant and 0.005 mmol of EDTA in 50 mL of water in carefully sealed 50-mL flasks. The solutions were stirred for 7 days at 26 °C and subsequently freeze-dried. The SDS- and CTAB-containing reaction mixtures were stirred with 100 mL of ether. After filtration and evaporation of the ether, crude **3c** was obtained as an oil.<sup>47</sup> The endo/exo ratios were determined using  $^1H$  NMR as described previously.<sup>9b</sup> Extraction of the Diels–Alder adducts from the freeze-dried reaction mixture containing  $C_{12}E_7$  was performed by stirring with 50 mL of pentane. Cooling the solution to  $-18$  °C resulted in precipitation of the surfactant. Filtration and evaporation of the solvent afforded the adduct mixture.<sup>47</sup>

**Kinetic Measurements.** All kinetic measurements were performed using UV–visible spectroscopy (Perkin-Elmer  $\lambda 2$ ,  $\lambda 5$ , or  $\lambda 12$  spectrophotometers) monitoring the decrease of the absorption of the dienophile at  $25 \pm 0.1$  °C. Two methods were used to determine the reported second-order rate constants. The rate constants of the fast reactions (half-lives not more than a few hours) were determined by following the reaction for 4–5 half-lifetimes. The rate constants for the slower reactions and the reactions with cyclopentadiene in aqueous solutions with half-lives of more than 15 min were determined using initial rate kinetics. Using the former method, the kinetic data were reproducible within 3%, whereas the data obtained using the initial rate technique were reproducible within 5%. Both methods have been described previously.<sup>9b</sup>

**NMR Measurements.** Routine spectra were taken on a Varian VXR 200- or 300-MHz spectrometer. The aromatic shift measurements and the paramagnetic relaxation measurements were performed on a Bruker AC 250-MHz spectrometer. Proton chemical shifts were determined relative to the signal of HOD (4.63 ppm). Paramagnetic relaxation times were determined using the inversion–recovery pulse sequence.<sup>42</sup> The variable delay times between the 180° and the 90° pulse were chosen so that they cover the relaxation process during the time span of minimally 5 times  $T_1$ . The 10–16 different delay times were in a random order to minimize systematic errors that might result from fluctuations of the strength of the magnetic field during the experiment. The delay time between subsequent pulse sequences was at least 5 times  $T_1$ . The  $T_1$  values were calculated using a least-squares fitting procedure available on the Varian software.

**Acknowledgment.** This work has been performed under the auspices of NIOK, Netherlands Institute for Catalysis Research, Lab Report 98-1-02. We gratefully acknowledge the Dutch Organization for Scientific Research (NWO) for a travel grant to S.O.

**Supporting Information Available:** Derivation of eq 1 (2 pages print/PDF). See any current masthead page for ordering information and Web access instructions.

(45) Fukushima, H.; Taylor, D. M. *Langmuir* **1995**, *11*, 3523.

(46) Value deviant due to the presence of a small amount of water in the hygroscopic crystals of **1f**.

(47) Repeating the extraction procedure did not change the endo–exo product ratio.